This article has been accepted for publication in IEEE/OSA Journal of Lightwave Technology. This is the author's version which has not been fully edited and content may change prior to final publication. Citation information: DOI 10.1109/JLT.2023.3240026

Compensation of Phase Noise Impairments in Distributed Acoustic Sensors based on Optical Pulse Compression Time-Domain Reflectometry

Enrique Piñeiro, Mikel Sagues, and Alayn Loayssa, *Senior Member, IEEE*

***Abstract*—We introduce a method to compensate for the deleterious effects of the phase noise of the laser source on long-range distributed acoustic sensors (DAS) that implement optical pulse compression (OPC). Pulse compression can be used in coherent optical time-domain reflectometry (COTDR) sensors to extend the measurement range without compromising spatial resolution. In fact, OPC-COTDR sensors have demonstrated the longest measurement range to date in passive sensing links that do not require distributed amplification to compensate fiber attenuation. However, it has been found that the limited coherence of the laser source has a degrading effect on the actual performance enhancement that pulse compression can bring because it constrains the maximum duration of the compression waveforms that can be used and makes the use of lasers with extremely low phase noise necessary. We introduce a technique to compensate for the effects of phase noise on OPC-COTDR sensors so that they can demonstrate their full potential for long-range measurements using lasers with less stringent phase noise requirements. The method is based on sampling the phase noise of the laser with an auxiliary interferometer and using this information in a simple signal processing technique to mitigate its deleterious effect on the signal measured. We test our method in an OPC-COTDR sensor that uses 500-μs linear frequency modulated pulses to demonstrate 100-km range measurements with 200 p$\epsilon/\sqrt{\text{Hz}}$ of strain sensitivity at 2-m initial spatial resolution that becomes 10-m after applying the gauge length. To our knowledge, this is the longest compression waveform demonstrated to date in an OPC-COTDR sensor. Its use provides an extra 20-km range compared to previous demonstrations using laser sources of comparable linewidth. Furthermore, comparable performance is also demonstrated when using a laser source with an order of magnitude larger linewidth.**

***Index Terms*—Phase Noise, Distributed Acoustic Sensing, Distributed Vibration sensing, Optical Pulse Compression, Optical Time Domain Reflectometry**

I. Introduction

DISTRIBUTED acoustic sensors (DAS) have been intensively researched in the last years [1]. These sensors take advantage of interferometric effects to detect and quantify small dynamic variations of the optical path length (OPL) in the fiber as a result of external excitation. One particular area that has attracted considerable interest is long-range DAS setups in which extremely small vibrations are detected along tens of kilometers of fiber optic cables. These have application for the monitoring of pipelines [2], electric power cables [3], road traffic [4], or seismic sources [5].

E. Piñeiro, M. Sagues, and A. Loayssa are with the Institute of Smart Cities and the Department of Electrical, Electronic, and Communications Engineering, Universidad Pública de Navarra, Pamplona 31006, Spain e-mail: alayn.loayssa@unavarra.es.

Several different DAS setups are suitable for these long-distance applications. For instance, direct-detection phase-sensitive optical time-domain reflectometry sensors, which are based on detecting changes in the amplitude of the backscattered signal from a particular position in the fiber as a result of excitations, have demonstrated long-range measurement capability [6], [7]. However, these sensors present a highly nonlinear response to excitation that makes it difficult to quantify the actual vibration in the fiber. Another method that also uses direct detection but provides quantification of the strain experienced by the fiber is based on using the dependence on wavelength of the interference coming from each location in the fiber and translating it to the time-domain by using chirped interrogation pulses [8]. One alternative to direct-detection schemes are coherent-detection methods that use a local oscillator to demodulate the full optical field (amplitude and phase) so that the changes in OPL between close locations in the fiber separated by a given gauge length can be determined by subtracting the phase of the backscattered signal from those locations [9]. This differential-phase coherent optical time-domain reflectometry (COTDR) setups have an intrinsic advantage for long-range applications because the measured backscattered signal is proportional to the amplitude of the optical field instead of its power; hence, it reduces with distance at half the rate than in direct-detection methods. Other long-range DAS proposals are also based on the differential-phase measurement, but implement the subtraction on the receiver side using an interferometer [10]. To achieve their ultimate distance reach, all of the above setups have deployed distributed amplification along the sensing fiber link to compensate for the fiber attenuation, which increases the system complexity.

Nevertheless, the DAS sensor type that has demonstrated to date the best capability to provide the longest possible range measurements in a purely passive link without additional distributed amplification is based on a refinement of the differential-phase COTDR setup in which optical pulse compression (OPC) is implemented [11], [12]. OPC is based on the same principles that have been applied for decades in radar systems but translated to the optical domain [13], [14]. In OPC, waveforms with long duration (high energy) and high time-bandwidth product are launched into the fiber so that the back-reflected signals can be processed upon reception with matched filters to produce narrow effective pulse widths. The whole range of compression waveforms developed for radar can be applied to OPC: from basic linear frequency

This article has been accepted for publication in IEEE/OSA Journal of Lightwave Technology. This is the author's version which has not been fully edited and content may change prior to final publication. Citation information: DOI 10.1109/JLT.2023.3240026

modulated (LFM) signals to complex pulse coded signals such as Golay or perfect periodic autocorrelation (PPA) sequences. OPC greatly relaxes the trade-off between spatial resolution and range in COTDR DAS sensors providing an enhancement in the measurement signal-to-noise ratio (SNR) that naturally leads to long-range measurements. The SNR improvement brought by OPC is, in principle, proportional to the increased duration (energy) of the compression waveform compared to the use of a simple pulse. However, early on, it was found that OPC performance was constrained by the phase noise of the laser source [13], [15], [16]. We have recently studied this effect in detail developing a theoretical model and finding that the sensitivity of OPC-COTDR degrades due to phase noise as the pulse duration is increased [17].

To our knowledge, no method has been demonstrated to date to compensate for the deleterious effect of the phase noise of the laser source on DAS sensors based on OPC-COTDR other than deploying lasers with extremely low phase noise, which tend to have higher costs or directly not be commercially available. In this work, we introduce a technique to compensate for the effects of the phase noise of the laser source so that OPC-COTDR can demonstrate its full potential for long-range measurements using lasers with less stringent phase noise requirements. The method is based on the use of an auxiliary interferometer to measure the phase noise of the laser source and a novel technique to take advantage of this information within the optical pulse compression processing to largely compensate its deleterious effects on the sensor performance.

We experimentally demonstrate our concept in a 100-km OPC-COTDR sensor that uses a 500 µs pulse compression waveform to achieve 200 $\mathrm{p}\epsilon/\sqrt{\mathrm{Hz}}$ of measurement sensitivity with 2-m spatial resolution. This is a 20-km improvement over previous setups that used a laser source with similar linewidth [11]. Furthermore, comparable performance is still obtained when the setup uses another laser source with an order of magnitude larger linewidth.

The use of auxiliary interferometers to compensate the phase noise of the laser source and measure its instantaneous frequency nonlinearity is an established practice in optical frequency-domain reflectometry [18], [19], [20], [21]. However, we are demonstrating here, for the first to our knowledge, its use in a time-domain reflectometry setup that uses optical pulse compression. Besides, as highlighted below, the processing required to leverage the measured phase noise is very different in OFDR than in OPC-COTDR sensors.

Previous efforts to compensate phase noise in other time-domain reflectometry systems can be found in the literature, but none in sensors using OPC for which the effects of the laser's phase noise are different than in conventional COTDR setups [17]. In [22], an interesting technique for compensating the optical path difference between reflections from the fiber and the local oscillator in a conventional, non-OPC, heterodyne-detection COTDR is introduced. Its principle is based on deploying a recirculating loop to obtain multiple delayed and frequency-shifted versions of the local oscillator that are simultaneously beaten with the back-reflected signals. However, this method does not scale well with fiber length since its requirements on the receiver bandwidth increase arithmetically with each recirculation. Furthermore, for long range measurements, the sensor performance would be degraded by the amplified spontaneous emission noise added at each recirculation by the erbium-doped fiber (EDFA) that compensates attenuation of the signal in the loop. Finally, in [23], there is another example of a COTDR system that aims to compensate the phase noise terms in the differential optical phase measured from consecutive reflectors in a quasi-distributed array. However, the method they propose is not valid for OPC-COTDR sensors in which the detrimental effects of phase noise manifest during pulse compression before any additional processing.

II. Fundamentals of the Phase Noise Compensation Technique

In OPC-COTDR sensors, the optical signal that is launched into the fiber can be expressed as [13], [17]:

$$E_{\mathrm{IN}}(t) = E(t)e^{j\phi(t)}e^{j\omega_0 t} \tag{1}$$

where $E(t)$ is the pulse compression waveform, which can be, for instance, an LFM pulse or a coded pulse sequence such as Golay [24] or PPA [25], ω_0 is the center radial optical frequency, and $\phi(t)$ represents the phase noise of the laser source. Then, the total optical signal reflected from the fiber is given by:

$$E_{\mathrm{OUT}}(t) = \int_0^T r(\tau_{rt})E_{\mathrm{IN}}(t-\tau_{rt})d\tau_{rt} \tag{2}$$

where $r\left(\tau_{rt}\right)$ is the random Rayleigh backscattering complex reflection coefficient for a position in the fiber with a roundtrip delay τ_{rt} to the origin, and T is the round-trip delay to the end of the fiber. This signal is detected in a coherent receiver with full I/Q demodulation followed by analog to digital conversion, which gives the complex signal:

$$A(t) = \int_0^T r(\tau_{rt})E(t-\tau_{rt})e^{j[\phi(t-\tau_{rt})-\phi(t)]}e^{j\omega_0\tau_{rt}}d\tau_{rt} \tag{3}$$

where terms such as detector responsivity have been obviated. The local oscillator used in the coherent detection is a sample of the original laser source obtained with a coupler. Notice that the detected signal includes a phase noise difference term due to the difference in propagation delay between the backscattered signals and the local oscillator paths. The received signal is then digitally cross-correlated with $E(t)$ to obtain the "compressed response", i.e., the measured complex backscatter profile of the sensing fiber, $\tilde{r}(\tau)$:

$$\tilde{r}(\tau) = (A \star E)(\tau) = \int_0^T r\left(\tau_{rt}\right) R(\tau, \tau_{rt})d\tau_{rt} \tag{4}$$

where $\star$ is the cross-correlation operator, and

$$R(\tau,\tau_{rt}) \equiv e^{j\omega_0\tau_{rt}} \int_{-\infty}^{+\infty} E^*(t-\tau)E(t-\tau_{rt})e^{j[\phi(t-\tau_{rt})-\phi(t)]}dt \tag{5}$$

This article has been accepted for publication in IEEE/OSA Journal of Lightwave Technology. This is the author's version which has not been fully edited and content may change prior to final publication. Citation information: DOI 10.1109/JLT.2023.3240026

Note that $R(\tau,\tau_{rt})$ is equivalent to the compressed response to an ideal perfect reflector positioned at a roundtrip delay of τ_{rt}. The time variable in (4) has been changed to $\tau \equiv 2z/v$ to denote the roundtrip time to a position z in the fiber with v group velocity.

If we assume that we are in the ideal situation in which the phase noise term in (3), can be neglected ($\psi_{\tau_{rt}}(t) \equiv \phi(t-\tau_{rt}) - \phi(t) \approx 0$), the compressed response becomes:

$$\tilde{r}(\tau) = \int_0^T r(\tau_{rt}) e^{j\omega_0 \tau_{rt}} R_{EE}(\tau - \tau_{rt}) d\tau_{rt} \tag{6}$$

where $e^{j\omega_0\tau_{rt}}$ is just a linear delay phase term, and

$$R_{EE}(\tau - \tau_{rt}) = \int_{-\infty}^{+\infty} E^*(t-\tau) E(t-\tau_{rt}) dt \tag{7}$$

Notice that $R_{EE}(t)$ refers to the auto-correlation of the transmitted compression waveform signal, $E(t)$. Therefore, with a well-chosen compression waveforms, $R_{EE}(t)$ becomes a narrow function of time and hence $\tilde{r}(\tau) \approx r(\tau_{rt})$, i.e. , the measured fiber response is approximately equal to its complex Rayleigh reflection coefficient as desired.

However, the differential phase noise term, $\psi_{\tau_{rt}}(t)$, can only be neglected for very short fiber links using very narrow-linewidth lasers. For longer ranges, the presence of this phase-noise-induced term leads to the deviation of the fiber's backscattered measurement from the ideal response and the introduction of the main penalty to the SNR and sensitivity of OPC-COTDR sensors [17].

Now, in order to explain the fundamentals of our phase-noise compensation technique, let's assume that we were able to measure $\psi_{\tau_{rt}}(t)$ for every τ_{rt}. In that case, it becomes possible to modify the OPC processing and compensate the phase noise degradation by cross-correlating the detected signal with $\tilde{E}(t) \equiv E(t) e^{j[\phi(t-\tau_{rt})-\phi(t)]}$, instead of just with $E(t)$, so that, in this case, the compensated compressed fiber response, $\tilde{\tilde{r}}(\tau)$, becomes:

$$\tilde{\tilde{r}}(\tau) = (A \star \tilde{E})(\tau) = \int_0^T r(\tau_{rt})\, e^{j\omega_0\tau_{rt}} R_{\tilde{E}\tilde{E}}(\tau - \tau_{rt}) d\tau_{rt} \tag{8}$$

with

$$R_{\tilde{E}\tilde{E}}(\tau - \tau_{rt}) = \int_{-\infty}^{+\infty} E^*(t-\tau) e^{-j[\phi(t-\tau)-\phi(t-\tau+\tau_{rt})]} \cdot E(t-\tau_{rt}) e^{j[\phi(t-\tau_{rt})-\phi(t)]} dt \tag{9}$$

Note that $R_{\tilde{E}\tilde{E}}(t)$ is now the autocorrelation of $\tilde{E}(t)$. Furthermore, in the positions of interest, close to the autocorrelation peak, $\tau \to \tau_{rt}$, and the phase noise terms in (9) cancel out. Hence, $R_{\tilde{E}\tilde{E}}(t) \approx R_{EE}(t)$ and, as in the ideal case without phase noise, $\tilde{\tilde{r}}(\tau) \approx r(\tau_{rt})$, hence the deleterious effects of the phase noise of the laser source are largely compensated.

However, measuring $\psi_{\tau_{rt}}(t)$ for every τ_{rt} is not simple. What we propose in our technique is to measure $\psi_{\tau_{rt}}(t)$ for a particular τ_{rt} by using the experimental setup in Fig. 1, which is described in detail in section III. This uses an auxiliary interferometer with a delay imbalance, $\tau_{aux} = L_{aux}/v$, provided by a length of fiber L_{aux}, so that the phase difference $\psi_{\tau_{aux}}(t) \equiv \phi(t-\tau_{aux}) - \phi(t)$ can be measured at the receiver associated to this interferometer. Then, the compensation works by correlating the received signal in the measurement channel with $E(t)e^{j\psi_{\tau_{aux}}(t)}$, using the phase noise obtained from the auxiliary interferometer. According to our previous discussion, this means that the phase noise effects for the reflections arriving from the position in the fiber under test $z_1 = L_{aux}/2$ can be compensated.

Furthermore, it is possible to deploy a modified version of the concatenated generated phase (CGP) method, which has been used in the past in the compensation of phase noise effects in optical frequency domain reflectometers [18]. In OFDR, this method is used to calculate the phase term of the signal of a reference interferometer with an integer multiple of the physical delay used. In our technique, we calculate the compensation phase difference for any integer multiple n of τ_{aux} by:

$$\psi_{n\tau_{aux}}(t) = \phi(t-n\tau_{aux}) - \phi(t) = \sum_{k=0}^{n-1} \psi_{\tau_{aux}}(t-k\tau_{aux}) \tag{10}$$

Therefore, with our technique and using a single simultaneous auxiliary interferometer measurement, we can compensate for the phase noise degradation for all positions in the fiber under test, $z_n = n \cdot L_{aux}/2$, that are at multiples of the round-trip delay of the auxiliary interferometer. Furthermore, as it is shown below, even in between z_n positions, phase noise compensation is achieved, although with reduced effectiveness.

Notice that, as mentioned in the introduction, the signal processing associated with the use of an auxiliary interferometer to compensate phase noise effects in our system for OPC-COTDR sensors and in OFDR systems is quite different. In OFDR, the detected signals contain the beat of a local and backscattered LFM optical signal, and the fiber response is obtained by applying a Fourier transformation. On the contrary, in OPC-COTDR multiple types of compression waveform can be deployed, not just LFM signals, and the fiber response is obtained, as was explained before, by cross-correlation. Moreover, there are two main methods to use an auxiliary interferometer to compensate phase noise in OFDR. One option is to sample the beat signal based on timing that corresponds to certain increments in the phase term of the reference signal of the auxiliary interferometer [18]. The other is to apply a so-called deskew filter that is only valid for linear frequency sweep signals [21]. These methods are not applicable to OPC-COTDR signals. What we introduce in this paper is a phase noise compensation method using an auxiliary interferometer that, for the first time to our knowledge, works for OPC-COTDR sensors.

This article has been accepted for publication in IEEE/OSA Journal of Lightwave Technology. This is the author's version which has not been fully edited and content may change prior to final publication. Citation information: DOI 10.1109/JLT.2023.3240026

III. Experimental Setup

Fig. 1 depicts the experimental setup that we have used to demonstrate our phase noise compensation technique. The upper branch is a conventional OPC-COTDR sensor setup in which a Mach-Zehnder electrooptic modulator (MZ-EOM) is used to generate the pulse compression waveform from a narrow linewidth laser [11], [12], [17]. Three different 1550-nm lasers were used in the experiments: an NKT Kosheras E15 with 100-Hz nominal linewidth, and two different RIO Orion modules with 2-kHz and 4.1-kHz linewidth, respectively. The MZ-EOM is biased for minimum transmission so that double-sideband with suppressed carrier signals are obtained in response to the application of RF sinusoidal signals. The signals driving the MZ-EOM are generated in an arbitrary waveform generator (AWG). For the experiments used in this paper, just LFM waveforms were used, but the setup can handle more complex compression waveforms such as PPA sequences [25].

The generated compression waveforms at the output of the MZ-EOM are amplified in an EDFA and launched into the fiber under test via a circulator. For the long-duration waveform used in these experiments, the limiting factor for the power launched into the fiber is the Brillouin scattering threshold [12]. Indeed, the maximum peak power of the compression waveform pulses, P_{peak}, that can be injected in a long fiber is related to the Brillouin gain, g_B, pulse duration, T_P, fiber's attenuation, α, effective area, A_{eff}, and a constant threshold parameter, θ, by the expression [26]:

$$g_B \frac{P_{peak}}{A_{eff}} \frac{(1 - e^{\alpha \frac{T_P}{2} v})}{\alpha} = \theta \tag{11}$$

Using this expression, it is simple to show that the maximum energy of the compression waveform that can be launched into a given fiber link, which is given by $P_{peak} \cdot T_P$, increases with its duration. Hence, it is convenient to use long-duration waveforms to increase the measurement SNR, provided that the phase noise impairments are compensated. In our experiments, the fiber under test was a 112.5-km length of standard single-mode fiber made of two 50-km spools followed by another of 12.5-km length. A 10-m piezoelectric fiber stretcher (PZT) was installed at the 100-km position, before the last fiber spool, to simulate excitation in the fiber. LFM pulses of 50-MHz peak-to-peak frequency modulation, 500-µs duration and 9-mW peak power were launched into the fiber.

The backscattered signals from the fiber are directed to a coherent receiver. Homodyne receivers made of a 90° optical hybrid coupler and balanced detectors are used in this implementation to enable the deployment of complex compression waveforms. However, for the LFM pulses that are used in our experiments, it would be possible to use heterodyne receivers instead and further simplify the setup. Furthermore, polarization diversity is not used in this proof-of-concept demonstration, but it is very simple to add using standard procedures.

The lower branch of the setup consists of the auxiliary interferometer for which a $L_{aux} = 5.4$ km fiber reel inserted inside an acoustic and vibration isolated enclosure is used. In principle, this interferometer could work in baseband, but to avoid DC-drift issues we inserted an acousto-optic modulator driven by a 100-MHz tone to implement a frequency shifter that leads to bandpass demodulation of the interferometer phase. Finally, the complex field measurements in the upper and lower interferometers are digitized and processed in a computer.

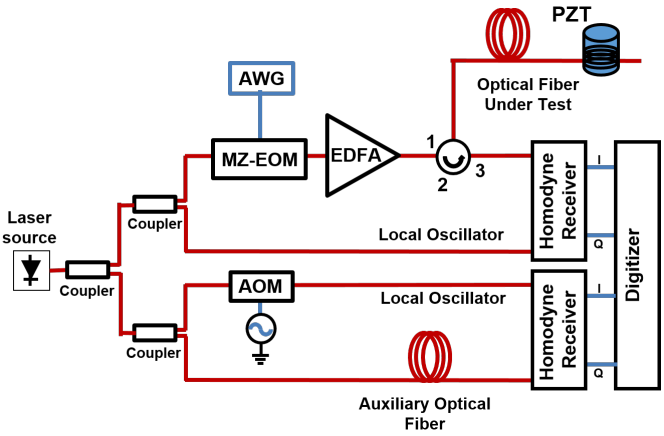

Fig. 1. Experimental setup of a time-domain DAS sensor with compensation of the phase noise of the laser. The upper branch of the setup is a long-range coherent OTDR that uses pulse compression. The lower branch consists of the auxiliary interferometer that samples the phase noise of the laser.

IV. Experimental Results

We start by illustrating the effect of the phase noise compensation on the detected signal in a simplified scenario in which a single reflection is measured from a remote location in the fiber. For this purpose, we momentarily removed from the setup in Fig. 1 the EDFA, circulator, and fiber under test, and inserted a ∼50-km fiber spool directly between the output of the MZ-EOM and the input to the receiver. Propagation of the compression waveform through this fiber length provides a signal equivalent to that of a reflection from a distance equal to half the length of the fiber, i.e., ∼25 km. Fig. 2 and Fig. 3 depicts the signal after pulse compression with and without phase noise compensation for several consecutive LFM pulses of 50-MHz peak-to-peak frequency modulation and 500-µs duration launched into the fiber. Fig. 2 (a) highlights the effect of the phase noise on the compressed waveform when the 100-Hz linewidth NKT laser was used. Notice that there seems to be some sort of "jitter" on the response for each consecutive pulse. This is due to the phase noise experienced by each pulse, which induces a Doppler-like effect. Indeed, each pulse experiences a phase modulation during its duration given by $\psi_{\tau_0}(t)$ with τ_0 the delay of the reflection. This can be also interpreted as a frequency modulation calculated by the derivative of the phase modulation, $\psi'_{\tau_0}(t)/(2\pi)$, which, due to the range-Doppler coupling that takes place with LFM pulse compression, translates into an apparent variation in the location of the reflection for each pulse depending on the random phase noise that it experiences. Fig. 2 (b) highlights the effects of applying the phase noise compensation processing to these same measurements. This is the result

This article has been accepted for publication in IEEE/OSA Journal of Lightwave Technology. This is the author's version which has not been fully edited and content may change prior to final publication. Citation information: DOI 10.1109/JLT.2023.3240026

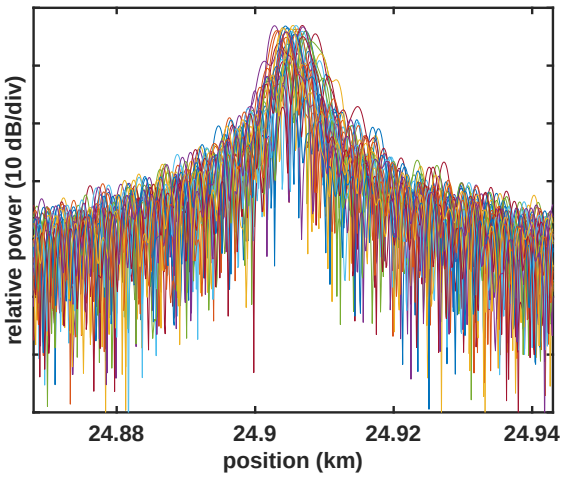

(a)

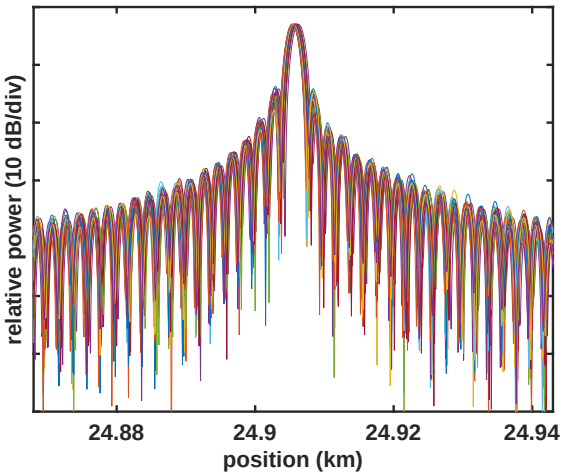

(b)

Fig. 2. Measured compressed response for a single reflection from a 25-km distance using a 100-Hz linewidth NKT laser source in the OPC-COTDR sensor setup (a) without and (b) with phase-noise compensation. An LFM compression waveform with 500-µs duration and 50-MHz bandwidth was deployed in this measurement.

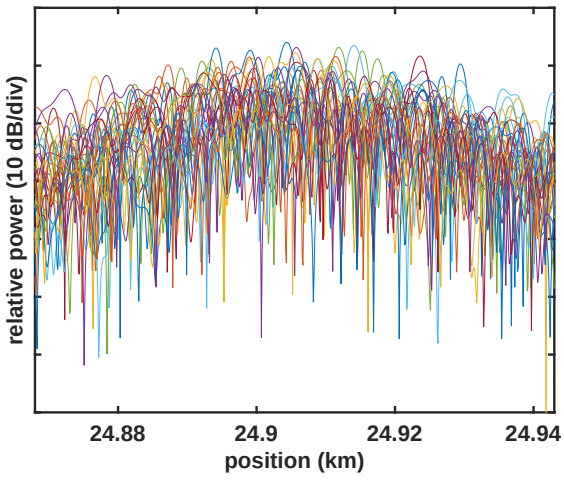

(a)

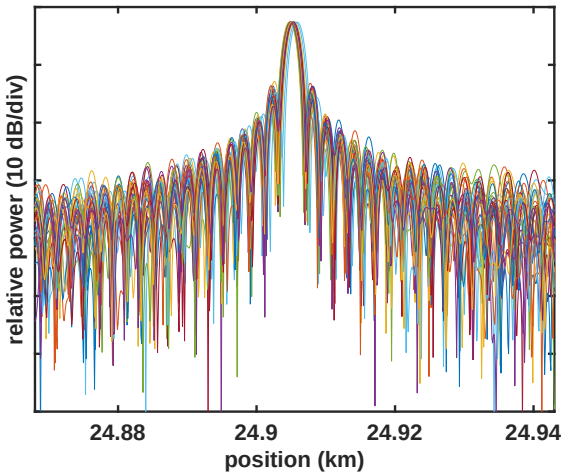

(b)

Fig. 3. Measured compressed response for a single reflection from a 25-km distance using a 4.1-kHz linewidth RIO laser source in the OPC-COTDR sensor setup (a) without and (b) with phase-noise compensation. An LFM compression waveform with 500-µs duration and 50-MHz bandwidth was deployed in this measurement.

of cross-correlating the detected signal with the ideal LFM signal multiplied by $e^{j\psi_{n\tau_{aux}}(t)}$ calculated using $n = 9$ in (10), which in this case is the integer multiple of the delay of the auxiliary fiber closest to the delay τ_0. The application of this processing largely removes the "jitter" of the compressed response with just some residual effect remaining due to the fact that $n\tau_{aux}$ is not exactly equal to τ_0. Fig. 3 depicts identical before-and-after comparison for the same measurement as before, but deploying the 4.1-kHz linewidth RIO laser instead. The phase noise compensation effects are even more dramatic in this case because, without compensation, the measurement has a larger distortion due to the increased phase noise of the laser. This agrees with our recent study on phase noise effects on OPC-COTDR sensors that highlighted that their severity increases with laser's linewidth, round-trip delay to the reflection, and duration of the compression waveform [17].

The effects of the laser phase noise on pulse compression depend on the particular compression waveform that is deployed. We have seen the "jitter"-like effect for LFM. However, for other waveforms, such as PPA sequences or phase codes, which have a thumbtack-shaped ambiguity function, the effect of the phase noise modulation experienced by the compression waveform sequence manifests mainly as a reduction in amplitude. Nevertheless, the compensation of the phase noise leads to a suppression of its deleterious effects on the pulse compression whatever their particular manifestation.

Fig. 2 (b) and Fig. 3 (b) also provide a measurement of the spatial resolution obtained after pulse compression. In this case, the 50-MHz sweep bandwidth (SBW) of the deployed LFM translates to ∼2-m (20-ns) spatial resolution as given by the theoretical $1/SBW$. Another observation from this figure is the main lobe to sidelobe ratio, which for LFM is measured to be around the theoretical ∼13 dB. The influence of this ratio on the performance of OPC-COTDR sensors has

This article has been accepted for publication in IEEE/OSA Journal of Lightwave Technology. This is the author's version which has not been fully edited and content may change prior to final publication. Citation information: DOI 10.1109/JLT.2023.3240026

not been investigated in-depth yet. In any case, this ratio can be increased by deploying well-known techniques borrowed from the radar realm, such as apodization [27] or the use of nonlinear FM [11], which are fully compatible with our phase-noise compensation technique.

After the single-reflection test, we reconnected the setup with the EDFA, circulator, and fiber under test to perform fully distributed DAS measurements. Fig. 4 (a) depicts the compressed backscattered signal profile obtained. Notice that at the end of the 112.5-km length of fiber there is still signal above the noise floor, suggesting that longer sensing lengths may be feasible in a further evolution of the setup. Also, note that positions with large Rayleigh signal fading are visible throughout the trace. These are mitigated with the signal processing explained below. The large enhancement in the detected signal due to the use of a long LFM pulse with OPC can be appreciated by comparing with the measurement in Fig. 4 (b), in which a conventional unmodulated 20-ns pulse has been deployed in the same setup to provide 2-m spatial resolution without OPC. The peak power of the pulse could be increased in this case to around 20 mW before the onset of significant modulation instability effects. Nevertheless, it is observed that the reflected signal becomes rapidly buried in the detection noise floor as we progress along the fiber.

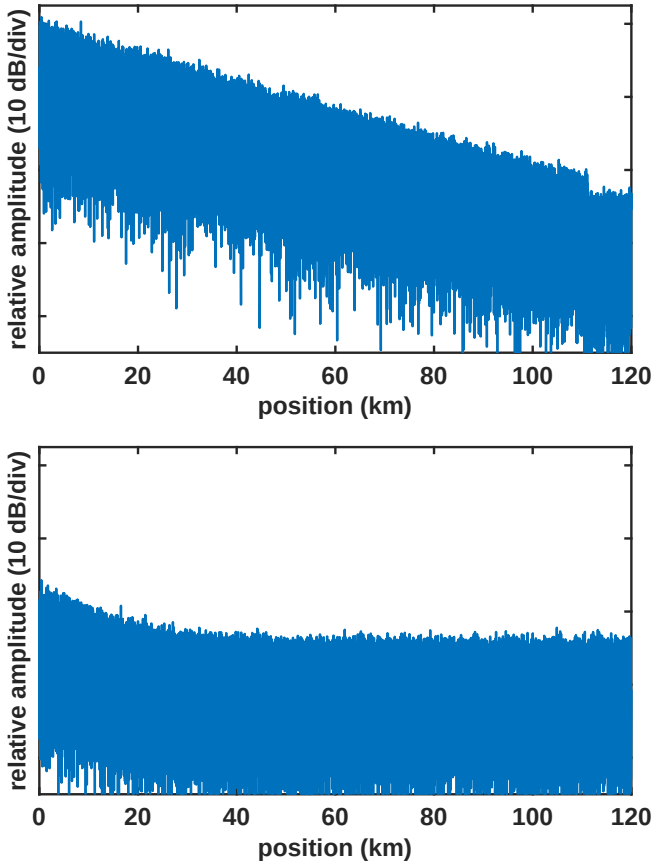

Fig. 4. Reflectivity signal for the 112-km OPC-COTDR sensor setup using either (a) an LFM compression waveform with 500-μs duration and 50-MHz bandwidth, or (b) a conventional 20-ns pulse.

The strain measurement with OPC-COTDR sensors is obtained using the differential-phase method in which the optical phase difference of the compressed backscattered field from positions separated by a given gauge length is calculated. This phase difference is proportional to the change in the optical path length induced by local strain in the fiber. To characterize the self-noise of the sensor, we measured the differential phase while the fiber under test was inside an acoustic and vibration-isolating enclosure. Then, we calculated the sensitivity of the sensor as the standard deviation of the measured noise for the full measurement bandwidth. This is depicted in Fig. 5 for the three different lasers that we had available: the 100-Hz linewidth NKT, and the 2-kHz and 4.1-kHz RIO modules. For these measurements, we used the same LFM pulses with 500-μs duration and 50-MHz peak-to-peak frequency deviation centered at 50-MHz that were used throughout all the experiments described in this paper. The signal processing that was implemented to arrive at the final measurements started by applying a matched filtering to the time-domain data to cross-correlate the backscattered signal with either the ideal compression waveform or the phase-noise compensated version according to the procedure outlined in section II. Then, we implemented the rotated-vector-sum method for fading compensation by calculating a 10-m moving average of the compressed backscattered optical field along the fiber [28]. The phase difference between positions separated by a gauge length of 10 m was calculated by integrating the phase increment between consecutive positions, which led to a simultaneous robust unwrapping of the total phase difference. Fig. 5 (a), and its enlarged view in Fig. 5 (b), highlight the sensitivity for the conventional system with no phase noise compensation. The sensitivity is good for short distances but it

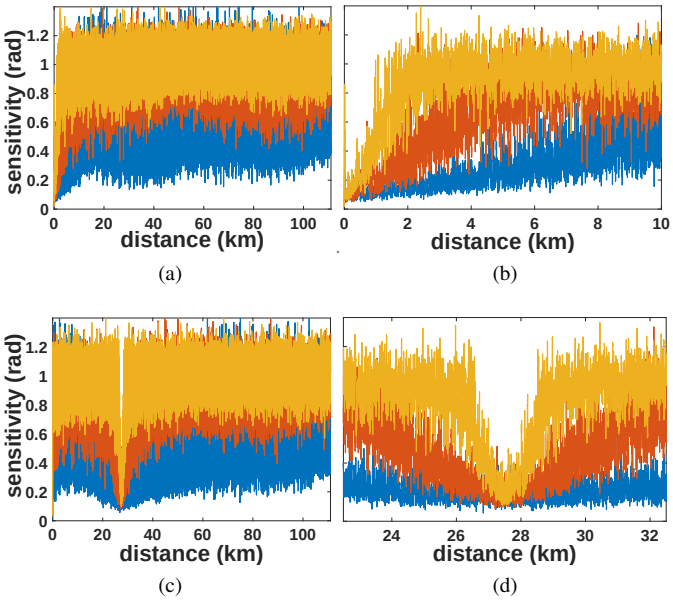

Fig. 5. Sensor sensitivity measured along the fiber under test when using three different laser sources with 100-Hz (blue lines), 2-kHz (red lines), and 4.1-kHz (yellow lines) linewidth (a) without and (c) with single-position phase noise compensation using the phase noise sampled for the $n = 10$ integer multiple of the auxiliary interferometer delay. Figures (b) and (d) display enlarged views of (a) and (c), respectively.

This article has been accepted for publication in IEEE/OSA Journal of Lightwave Technology. This is the author's version which has not been fully edited and content may change prior to final publication. Citation information: DOI 10.1109/JLT.2023.3240026

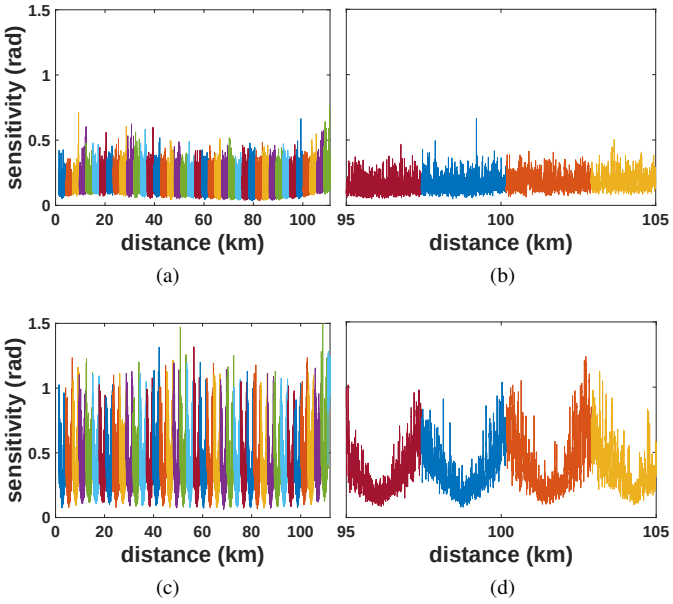

Fig. 6. Sensitivity vs. position after full fiber phase noise compensation for the setup using the (a) 100-Hz linewidth NKT laser or (c) 4.1-kHz RIO laser. The fiber segments compensated using the phase noise sampled for consecutive integer multiples of the auxiliary interferometer delay calculated with the CGP method are displayed with different colors. Figures (b) and (d) display enlarged views of (a) and (c), respectively.

steadily degrades as the backscatter distance increases, which is consistent with the trends that were mentioned before. This means that vibration measurements at long distances are not feasible, as will be shown below. Moreover, as expected, the larger the linewidth, the faster the sensitivity degradation. Also notice that the sensitivity degradation tends to saturate to a maximum value for a large enough distance. However, this apparent saturation is just a consequence of the fact that the phase difference is a modulo-2π quantity; hence, its standard deviation is going to be bound even when it is applied to purely random complex signals of very large variance. In fact, these same saturated sensitivity values were obtained when we applied our signal processing to the noise floor of the compressed backscattered measurements outside the fiber range. Fig. 5 (c) and (d) depict the same measurement when phase noise compensation processing is applied using the phase $\psi_{\tau_{rt}}(t)$ measured with the auxiliary interferometer. In this case, we are using the CGP method of (10) to compensate the phase noise, but just using the $n = 10$ integer multiple of the auxiliary interferometer delay, i.e., $\psi_{10\tau_{aux}}(t)$. Notice that the effect of the compensation is a sort of "reset" of the phase noise. At the exact compensation location, the sensitivity is optimized but at nearby locations, it again degrades following the same general profile that was observed at the start of the fiber when no compensation was deployed. Furthermore, it can be seen that the best sensitivity at the optimum compensation position is similar for the three different lasers. Their difference in terms of phase noise performance manifests in the width of the enhanced sensitivity region, which is larger the lower the linewidth of the laser used.

Fig. 6 demonstrates full-fiber compensation when the sensor uses either the laser source with the smallest or largest linewidth, i.e., 100-Hz NKT or 4.1-kHz RIO. As shown in Fig. 5, the compensation of the phase noise effects that our technique provides is very good at the specific $z_n = nL_{aux}/2$ locations, almost equal to the sensitivity at the start of the fiber for the uncompensated case. Furthermore, there is also a good compensation in the vicinity of these locations because $\psi_{n\tau_{aux}}(t)$ is still a good approximation to the phase noise that the compression waveforms backscattering from those locations experience. In the fully compensated sensor, the fiber under test is divided into equal-length segments around each z_n, i.e., $L_{aux}(n/2 - 1/4) < z < L_{aux}(n/2 + 1/4)$, in which the cross-correlation using $E(t)e^{j\psi_{n\tau_{aux}}(t)}$ is applied. Each segment is displayed with a different color line in Fig. 6. Given the length of the auxiliary interferometer and the width of the compensated area, it is found that for the NKT laser there is very good overlapping between consecutive segments so that the sensitivity remains good through the fiber length. For the RIO laser, the width of each "compensation valley" is narrower so that the sensitivity is seen to degrade in between segments. To avoid this issue, a shorter length of fiber could be used in the auxiliary interferometer to reduce the length of each compensation segment. However, it was found that when short lengths of auxiliary fiber were used, the compensation degraded as the integer multiple used in the CGP method increased. This is attributed to the deficiencies of the isolation of the auxiliary fiber spool that we were able to achieve. This isolation is very important because any vibration noise picked by this fiber is multiplied by the CGP procedure. In any case, the full-bandwidth average sensitivity along the fiber length was found to be of the same order for the NKT (0.1653 rad) and the RIO (0.3842 rad) lasers.

After characterizing the sensitivity improvement provided by our phase-compensation technique we demonstrated its operation with actual excitation in the fiber. Sinusoidal signals were applied to the PZT at the 100-km location. Fig. 7(a) and (b) depicts the time-domain differential phase measured at the fiber after applying the phase noise compensation technique for the two laser sources, NKT and RIO. It can be seen that the excitation is measured with a clear definition in both position and time. The quality of the measurement is good for the two laser sources deployed, being slightly better for the narrower linewidth NKT than for the RIO. Note that without compensation, as Fig. 7(c) highlights, the measurement was found to be completely distorted and the excitation signal could not be discerned whatsoever. For these measurements, the phase difference was directly calculated from positions separated by a length of 20 m so that it extended beyond the 10-m length of the PZT.

The total measured time in these excitation measurements was 0.23 s, with a slow-time sampling frequency of 1.8 ms and 128 compression waveforms launched into the fiber, yielding 1.765 million samples acquired per waveform (with a spatial sampling of 10 cm). The total processing time for this time segment, using a desktop computer running a Matlab script, was 155 s, including 67 s to calculate the compensating phase difference term and 76 s for the cross-correlation. However, there is ample potential for reducing these times, as

This article has been accepted for publication in IEEE/OSA Journal of Lightwave Technology. This is the author's version which has not been fully edited and content may change prior to final publication. Citation information: DOI 10.1109/JLT.2023.3240026

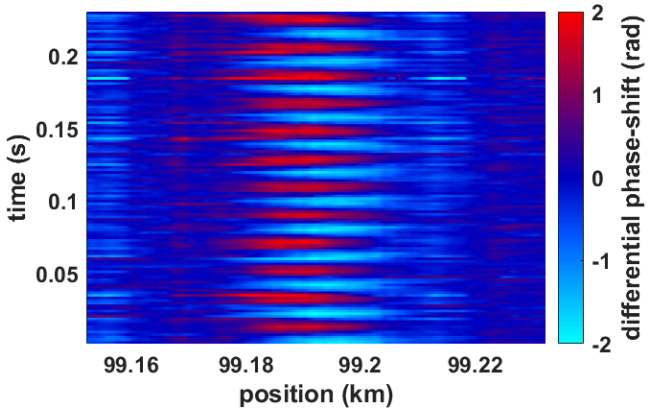

(a)

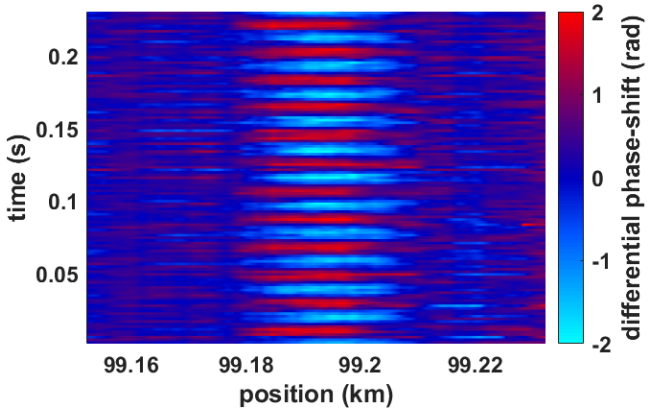

(b)

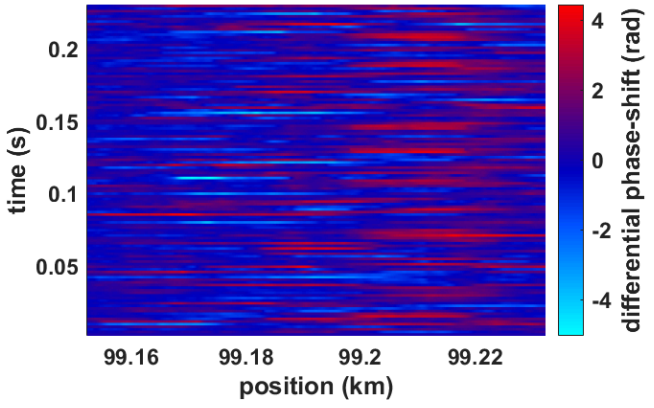

(c)

Fig. 7. Time-domain differential phase measured after phase-noise compensation for the setup using either (a) the 100-Hz linewidth NKT laser or (b) the 4.1-kHz linewidth RIO laser when a 52-Hz sinusoidal is applied to the PZT at the 100-km distance. Also shown in (c) is the measurement without phase-noise compensation for the NKT.

all the mathematical operations involved can be accelerated through the use of specialized hardware such as graphics processing units (GPUs) or field-programmable gate arrays (FPGAs).

Fig. 8 shows the calculated spectrum for the differential phase measured at the PZT location for several excitation

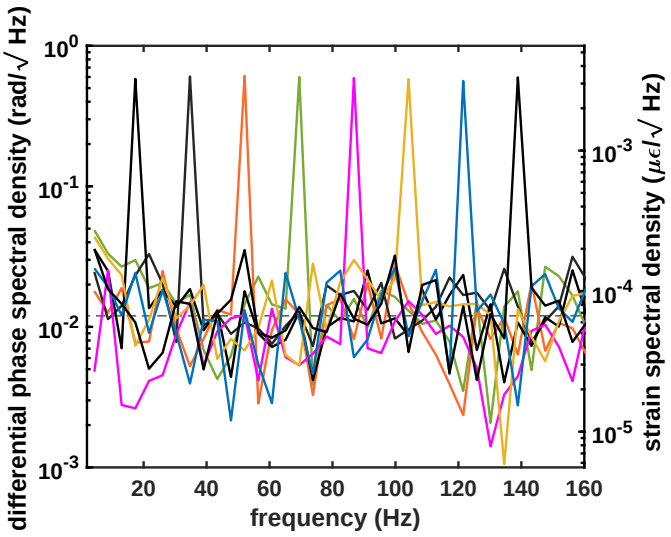

Fig. 8. Spectral density of the measured signal for a sweep of the excitation frequency.

frequencies, where a flat frequency response and nonlinear distortion-free measurements can be appreciated. The measurements with the RIO laser are depicted here. Clean peaks ∼30 dB above the noise floor are obtained. In addition, the noise floor in this measurement gives the spectral density of the sensitivity, which was found to be ∼20 mrad/$\sqrt{\text{Hz}}$ which would translate to ∼200 p$\epsilon/\sqrt{\text{Hz}}$ in terms of actual strain in the fiber for a 10-m gauge length.

The maximum slow-time sampling frequency for these measurements is around 600 Hz taking into account the 1.12 ms of round-trip delay to the end of the fiber and another 500 µs from the LFM pulse duration. This sampling frequency could be increased, for instance, by using PPA codes as compression waveform, for which cyclic convolution is used and the sequence repetition period can be equal to the fiber's round-trip delay [25].

V. Conclusions

In summary, we have demonstrated that our technique provides compensation for the sensitivity degradation induced by the laser source in OPC-COTDR sensors. Using this method we have been able to reach a range of 100 km, an extra of 20 km compared to previous demonstrations of OPC-COTDR sensors that used a similar laser source with 100-Hz nominal linewidth [11]. Furthermore, comparable performance has also been demonstrated when using a laser source with 4.1-kHz linewidth, an order of magnitude larger. This improvement has been made possible by our deployment of the longest compression waveform demonstrated to date in a long-range OPC-COTDR system. Previous long-range OPC-COTDR sensor demonstrations that have achieved longer lengths have required the use of lasers with better coherence than the ones used here [12]. The use of such narrow linewidth was needed in these other systems to mitigate the performance impairments brought by the phase noise of the laser. However, even with these enhanced lasers, the longest duration pulse demonstrated to our knowledge for long-range OPC-COTDR

sensors has been 100 µs. This duration was likely limited by the laser's phase noise, which increases its deleterious effects as the pulse compression waveform extends in time. In comparison, our experiments have demonstrated the use of a long 500-µs LFM pulses that can fill the fiber. This is significant since for OPC-COTDR sensors the SNR enhancement is proportional to the compression waveform duration.

Finally, we would like to mention that our technique serves to compensate the phase noise that the compression waveform signal experiences during its duration. Compensation of effects of possible slow longer-term drifts of the frequency of the laser on the COTDR sensor measurements have been reported elsewhere [29], [30].

ACKNOWLEDGMENT

The authors would like to thank Prof. Avishay Eyal for fruitful discussions. This work was supported in part by European Union "Next generationEU"/PRTR and MCIN/AEI/10.13039/501100011033 under grant PDC2021-121172-C21, in part by FEDER "A way to make Europe" and MCIN/AEI/10.13039/501100011033 under grant PID2019-107270RB-C22, and in part by Gobierno de Navarra under grant PC210-211 FIBRATRAFIC.

REFERENCES

[1] X. Bao, D.-P. Zhou, C. Baker, and L. Chen, "Recent development in the distributed fiber optic acoustic and ultrasonic detection," *Journal of Lightwave Technology*, vol. 35, no. 16, pp. 3256–3267, 2017.

[2] M.-T. Hussels, S. Chruscicki, D. Arndt, S. Scheider, J. Prager, T. Homann, and A. K. Habib, "Localization of transient events threatening pipeline integrity by Fiber-Optic distributed acoustic sensing," *Sensors (Basel)*, vol. 19, no. 15, Jul. 2019.

[3] Q. Che, H. Wen, X. Li, Z. Peng, and K. P. Chen, "Partial discharge recognition based on optical fiber distributed acoustic sensing and a convolutional neural network," *IEEE Access*, vol. 7, pp. 101 758–101 764, 2019.

[4] E. Catalano, A. Coscetta, E. Cerri, N. Cennamo, L. Zeni, and A. Minardo, "Automatic traffic monitoring by φ-OTDR data and hough transform in a real-field environment," *Appl. Opt.*, vol. 60, no. 13, pp. 3579–3584, May 2021.

[5] M. R. Fernández-Ruiz, H. F. Martins, E. F. Williams, C. Becerril, R. Magalhães, L. Costa, S. Martin-Lopez, Z. Jia, Z. Zhan, and M. González-Herráez, "Seismic monitoring with distributed acoustic sensing from the near-surface to the deep oceans," *Journal of Lightwave Technology*, vol. 40, no. 5, pp. 1453–1463, 2022.

[6] F. Peng, H. Wu, X.-H. Jia, Y.-J. Rao, Z.-N. Wang, and Z.-P. Peng, "Ultra-long high-sensitivity ϕ-OTDR for high spatial resolution intrusion detection of pipelines," *Opt. Express*, vol. 22, no. 11, pp. 13 804–13 810, Jun 2014.

[7] H. F. Martins, S. Martin-Lopez, P. Corredera, J. D. Ania-Castañon, O. Frazão, and M. Gonzalez-Herraez, "Distributed vibration sensing over 125 km with enhanced snr using ϕ-OTDR over a URFL cavity," *Journal of Lightwave Technology*, vol. 33, no. 12, pp. 2628–2632, 2015.

[8] J. Pastor-Graells, H. F. Martins, A. Garcia-Ruiz, S. Martin-Lopez, and M. Gonzalez-Herraez, "Single-shot distributed temperature and strain tracking using direct detection phase-sensitive OTDR with chirped pulses," *Opt. Express*, vol. 24, no. 12, pp. 13 121–13 133, Jun 2016.

[9] D. Chen, Q. Liu, and Z. He, "108-km distributed acoustic sensor with 220-p$\varepsilon/\sqrt{\text{hz}}$ strain resolution and 5-m spatial resolution," *Journal of Lightwave Technology*, vol. 37, no. 18, pp. 4462–4468, 2019.

[10] A. Masoudi, M. Beresna, and G. Brambilla, "152 km-range single-ended distributed acoustic sensor based on inline optical amplification and a micromachined enhanced-backscattering fiber," *Opt. Lett.*, vol. 46, no. 3, pp. 552–555, Feb 2021.

[11] J. Zhang, H. Wu, H. Zheng, J. Huang, G. Yin, T. Zhu, F. Qiu, X. Huang, D. Qu, and Y. Bai, "80 km fading free phase-sensitive reflectometry based on multi-carrier NLFM pulse without distributed amplification," *Journal of Lightwave Technology*, vol. 37, no. 18, pp. 4748–4754, 2019.

[12] O. H. Waagaard, E. Rønnekleiv, A. Haukanes, F. Stabo-Eeg, D. Thingbø, S. Forbord, S. E. Aasen, and J. K. Brenne, "Real-time low noise distributed acoustic sensing in 171 km low loss fiber," *OSA Continuum*, vol. 4, no. 2, pp. 688–701, Feb 2021.

[13] W. Zou, S. Yang, X. Long, and J. Chen, "Optical pulse compression reflectometry: proposal and proof-of-concept experiment," *Opt. Express*, vol. 23, no. 1, pp. 512–522, Jan 2015.

[14] S. Wang, X. Fan, Q. Liu, and Z. He, "Distributed fiber-optic vibration sensing based on phase extraction from time-gated digital OFDR," *Opt. Express*, vol. 23, no. 26, pp. 33 301–33 309, Dec 2015.

[15] S. Wang, W. Zou, X. Long, and J. Chen, "Influence of phase noise on measurement range in optical pulse compression reflectometry," in *2015 Opto-Electronics and Communications Conference (OECC)*, 2015, pp. 1–3.

[16] E. Awwad, C. Dorize, S. Guerrier, and J. Renaudier, "Detection-localization-identification of vibrations over long distance SSMF with coherent $\delta\phi$-OTDR," *Journal of Lightwave Technology*, vol. 38, no. 12, pp. 3089–3095, 2020.

[17] A. Loayssa, M. Sagues, and A. Eyal, "Phase noise effects on phase-sensitive OTDR sensors using optical pulse compression," *Journal of Lightwave Technology*, vol. 40, no. 8, pp. 2561–2569, 2022.

[18] X. Fan, Y. Koshikiya, and F. Ito, "Phase-noise-compensated optical frequency domain reflectometry with measurement range beyond laser coherence length realized using concatenative reference method," *Opt. Lett.*, vol. 32, no. 22, pp. 3227–3229, Nov 2007.

[19] F. Ito, X. Fan, and Y. Koshikiya, "Long-range coherent OFDR with light source phase noise compensation," *Journal of Lightwave Technology*, vol. 30, no. 8, pp. 1015–1024, 2012.

[20] O. Y. Sagiv, D. Arbel, and A. Eyal, "Correcting for spatial-resolution degradation mechanisms in OFDR via inline auxiliary points," *Opt. Express*, vol. 20, no. 25, pp. 27 465–27 472, Dec 2012.

[21] Z. Ding, X. S. Yao, T. Liu, Y. Du, K. Liu, J. Jiang, Z. Meng, and H. Chen, "Compensation of laser frequency tuning nonlinearity of a long range OFDR using deskew filter," *Opt. Express*, vol. 21, no. 3, pp. 3826–3834, Feb 2013.

[22] M. Zabihi, X. Chen, T. Zhou, J. Liu, F. Wang, Y. Zhang, and X. Zhang, "Compensation of optical path difference in heterodyne ϕ-OTDR systems and SNR enhancement by generating multiple beat signals," *Opt. Express*, vol. 27, no. 20, pp. 27 488–27 499, Sep 2019.

[23] M. Wu, X. Fan, Q. Liu, and Z. He, "Highly sensitive quasi-distributed fiber-optic acoustic sensing system by interrogating a weak reflector array," *Opt. Lett.*, vol. 43, no. 15, pp. 3594–3597, Aug 2018.

[24] C. Dorize, E. Awwad, and J. Renaudier, "High sensitivity φ-OTDR over long distance with polarization multiplexed codes," *IEEE Photonics Technology Letters*, vol. 31, no. 20, pp. 1654–1657, 2019.

[25] J. J. Mompó, L. Shiloh, N. Arbel, N. Levanon, A. Loayssa, and A. Eyal, "Distributed dynamic strain sensing via perfect periodic coherent codes and a polarization diversity receiver," *J. Lightwave Technol.*, vol. 37, no. 18, pp. 4597–4602, Sep 2019.

[26] G. L. Keaton, M. J. Leonardo, M. W. Byer, and D. J. Richard, "Stimulated brillouin scattering of pulses in optical fibers," *Opt. Express*, vol. 22, no. 11, pp. 13 351–13 365, Jun 2014.

[27] J. J. Mompó, S. Martín-López, M. González-Herráez, and A. Loayssa, "Sidelobe apodization in optical pulse compression reflectometry for fiber optic distributed acoustic sensing," *Opt. Lett.*, vol. 43, no. 7, pp. 1499–1502, Apr 2018.

[28] D. Chen, Q. Liu, and Z. He, "Phase-detection distributed fiber-optic vibration sensor without fading-noise based on time-gated digital OFDR," *Opt. Express*, vol. 25, no. 7, pp. 8315–8325, Apr 2017.

[29] Q. Yuan, F. Wang, T. Liu, Y. Liu, Y. Zhang, Z. Zhong, and X. Zhang, "Compensating for influence of laser-frequency-drift in phase-sensitive OTDR with twice differential method," *Opt. Express*, vol. 27, no. 3, pp. 3664–3671, Feb 2019.

[30] M. Zabihi and K. Krebber, "Laser source frequency drift compensation in ϕ-OTDR systems using multiple probe frequencies," *Opt. Express*, vol. 30, no. 11, pp. 19 990–19 998, May 2022.